MatchDet: A Collaborative Framework for Image Matching and Object Detection

Jinxiang Lai[*1], **Wenlong Wu**[*1], **Bin-Bin Gao**[†1], **Jun Liu**[1], **Jiawei Zhan**[1], **Congchong Nie**[1], **Yi Zeng**[1], **Chengjie Wang**[†1, 2]

[1] Tencent Youtu Lab, China
[2] Shanghai Jiao Tong University, China
layjins1994@gmail.com, ezrealwu@tencent.com, {csgaobb, junsenselee}@gmail.com, {gavynzhan, nickccnie, sylviazeng}@tencent.com, jasoncjwang@tencent.com

Abstract

Image matching and object detection are two fundamental and challenging tasks, while many related applications consider them two individual tasks (i.e. task-individual). In this paper, a collaborative framework called MatchDet (i.e. task-collaborative) is proposed for image matching and object detection to obtain mutual improvements. To achieve the collaborative learning of the two tasks, we propose three novel modules, including a Weighted Spatial Attention Module (WSAM) for Detector, and Weighted Attention Module (WAM) and Box Filter for Matcher. Specifically, the WSAM highlights the foreground regions of target image to benefit the subsequent detector, the WAM enhances the connection between the foreground regions of pair images to ensure high-quality matches, and Box Filter mitigates the impact of false matches. We evaluate the approaches on a new benchmark with two datasets called Warp-COCO and miniScanNet. Experimental results show our approaches are effective and achieve competitive improvements.

Introduction

Image matching (Shrivastava et al. 2011) and object detection (Liu et al. 2020) are two fundamental and challenging tasks in computer vision. Image matching finds pixel-wise correspondences between image pairs, and object detection seeks to locate and classify object instances in images. With the combination of them, there are numerous important applications, including robot vision, autonomous driving, and industrial defect inspection. In robot vision and autonomous driving, it usually uses image matching technique to perform Simultaneous Localization And Mapping (SLAM) (Mur-Artal, Montiel, and Tardos 2015), and also needs to find the target category objects (e.g. pedestrian in autonomous driving) in images based on object detection technique. In industrial defect inspection, it applies image matching for registration (Shrivastava et al. 2011) to obtain Region-of-Interest (ROI), and then detects the target defects. The aforementioned applications consider image matching and object detection as two individual tasks (i.e. task-individual).

In this paper, a collaborative framework called MatchDet (i.e. task-collaborative) is proposed for image matching and

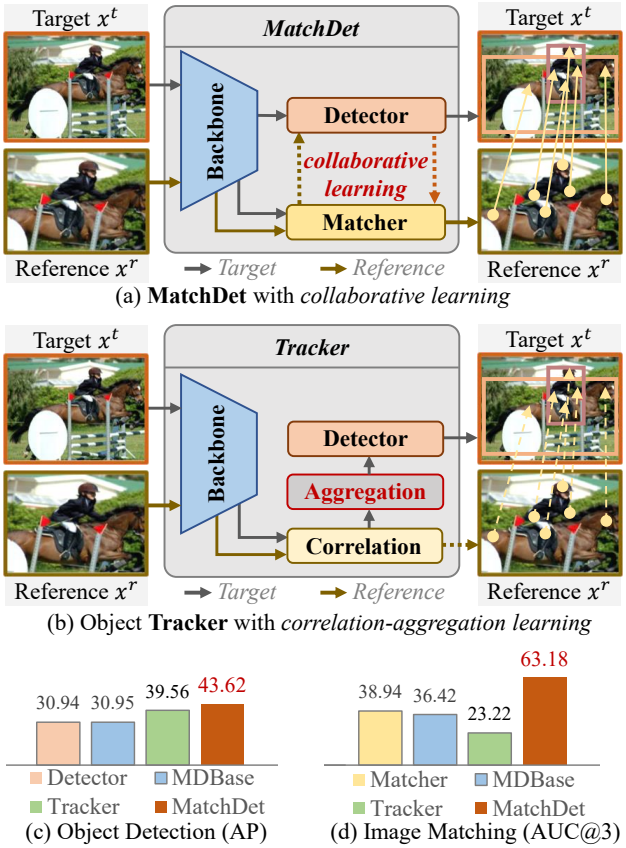

Figure 1: (a) Our MatchDet with collaborative learning for improving image matching and object detection. We introduce a baseline named MDBase network, which removes the collaborative learning module of MatchDet. (b) The object Tracker with correlation-aggregation learning. The dashed line represents that the Tracker has the potential ability to obtain pairwise correspondences, while there is no matching objective function to supervise it. (c) and (d) are the results on Warp-COCO dataset. (c) Our MatchDet obtains 4.06% improvement in object detection. (d) Our MatchDet achieves 24.24% higher performance in image matching.

[*]These authors contributed equally.
[†]Corresponding Author

object detection to obtain mutual improvements. As illustrated in Fig.1(a), given input reference and target images, our MatchDet simultaneously outputs their homography relationship and object detection results of the target image, which is defined as a Match-and-Detection task. The proposed MatchDet framework consists of a shared backbone, and two Matcher and Detector task branches for image matching and object detection, which is co-trained end-to-end. Under task-collaborative MatchDet framework, the homography relationship estimated by Matcher and the bounding boxes predicted by Detector can be useful to each other.

As presented in Fig.1(b), the most relevant approach is the correlation based Tracker (Christoph, Axel, and Andrew 2017) for the object tracking task. The Tracker utilizes the Correlation module to explore the affinity between the target image and the reference image, then further applies the Aggregation module to refine the affinity for enhancing the target objects. There are two main differences between MatchDet and Tracker: (i) MatchDet integrates a Matcher branch, which is able to obtain a precise homography relationship. However, Tracker only adopts the Correlation module to implicitly explore the affinity without the supervision of matching objective function, which leads to an imprecise homography relationship. As illustrated in Fig.1(d), our MatchDet achieves a large improvement with 39.96% in image matching task. (ii) MatchDet achieves mutual performance improvements in the two tasks via the proposed collaborative learning module, while Tracker only utilizes correlation-aggregation learning to improve the performance of the object detection task.

To achieve mutual performance improvements via the collaborative learning of the two tasks, we propose three novel modules, including a Weighted Spatial Attention Module (WSAM) for Detector, Weighted Attention Module (WAM) and Box Filter for Matcher. For Matcher branch, the proposed WAM produces more discriminative feature representations of image pairs, via learning global context to find the correspondences among surrounding regions, with the usage of Transformer structure (Sun et al. 2021). Benefiting from the Match-and-Detection task, it's achievable to obtain the potential foreground regions of images. Then the WAM can be more focus on interacting information among the foreground regions of pairs, which reduces background interference and ensures high-quality matches. Specifically, the WAM first utilizes a Weights Generator to generate weighted maps based on the foreground regions, and then uses the weighted maps to enhance the affinity matrix between feature pairs as implementing in the Attention operation of Transformer. Further more, Box Filter reduces the impact of the potential low-quality matches, via strengthening the matching scores among the foreground regions of pairs, where the foregrounds are predicted by Detector.

For Detector branch, the proposed WSAM, a variant of WAM, highlights the foreground regions of target image, via the similar regions with instance feature of reference image and learnable semantic embedding. To achieve the above purpose of enhancing foregrounds, the WSAM adopts Weighted Spatial Attention instead of Weighted Attention applied in WAM, and their essential difference is discussed in APPENDIX. Similar to WAM, the WSAM also pays more attention on feature interaction among foregrounds. The WSAM transforms the foreground regions of reference image with the homography estimated by Matcher, to generate the potential foreground regions for target image.

In general, our main contributions are:

• For the first time, we propose a collaborative framework called MatchDet for image matching and object detection to obtain mutual improvements. Besides, our MatchDet is a general framework, which can utilize different detectors such as FCOS, Faster-RCNN, and AdaMixer.

• To achieve collaborative learning of image matching and object detection, three novel modules are proposed, including a Weighted Spatial Attention Module (WSAM) which highlights the foreground regions of target image for Detector, and Weighted Attention Module (WAM) and Box Filter which obtains high-quality matches for Matcher.

• We evaluate the Match-and-Detection task on a new benchmark with two datasets called Warp-COCO and miniScanNet. This benchmark can be used to verify the performances of the algorithms on both image matching and object detection. Experimental results show our approaches are effective and achieve competitive improvements.

Related Work

Object Detection The current object detection algorithms can be divided into anchor-based (Ren et al. 2015; Redmon and Farhadi 2018; Lin et al. 2017; Zhang et al. 2019, 2020), anchor-free (Law and Deng 2018; Duan et al. 2019; Tian et al. 2019), and query-based (Carion et al. 2020; Gao et al. 2022; Zhang et al. 2023) methods. In this paper, we choose the classical anchor-free FCOS (Tian et al. 2019) as the basic detector due to its good performance and simplicity.

Image Matching Image matching finds pixel-wise correspondences between image pairs, with two main directions of Interest Point Detector-based (IPD-based) methods (Rublee et al. 2011; DeTone, Malisiewicz, and Rabinovich 2018) and IPD-free methods (Sun et al. 2021; Chen et al. 2022; Huang et al. 2023). In this paper, we choose the classical IPD-free LoFTR (Sun et al. 2021) as the basic image matcher due to its good performance and simplicity.

Transformer Attention The transformer Cross Attention in LoFTR (Sun et al. 2021) learns global context based on the full affinity matrix between feature pairs, but it may easily be distracted by background and causes the slow convergence of model. To alleviate this problem, we propose two novel transformer-based weighted attention and weighted spatial attention modules to strengthen the target object.

Problem Definition

The Match-and-Detection task aims to obtain the homography relationship and object detection results of the input pair images. Formally, given the pair images x^t and x^r, the Match-and-Detection method predicts the homography matrix $\hat{\mathcal{H}}$ and bounding boxes $\{\hat{B}_i^t\}$ for x^t. We denote x^t and x^r as the target and reference images respectively, the homography matrix $\mathcal{H} \in \mathbb{R}^{3\times3}$ represents their geometric

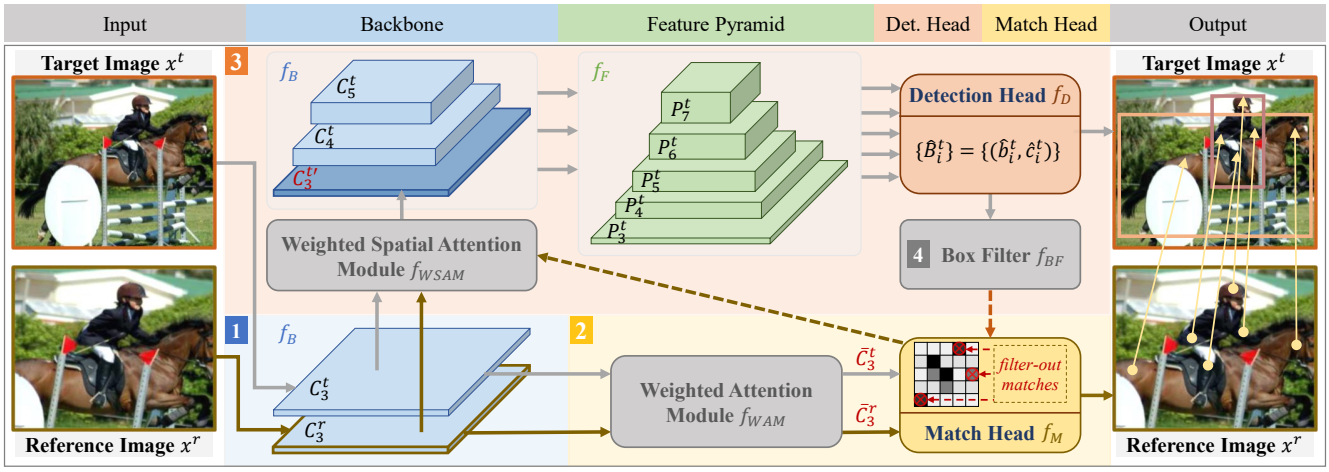

Figure 2: The network architecture of our MatchDet. There are four stages: ① Obtaining basic features $\{C_3^t, C_3^r\}$ with a shared backbone. ② Matcher branch estimates the homography matrix with the enhanced features $\{\bar{C}_3^t, \bar{C}_3^r\}$ produced by Weighted Attention Module. ③ Detector branch predicts the bounding boxes based on the highlighted features $C_3^{t\prime}$ generated by Weighted Spatial Attention Module. ④ Box Filter refines the image matching results via filtering out the potential mismatches.

relationship as $x^t = \mathcal{H}x^r$, and their ground-truth bounding boxes are defined as $\{B_i^t\}$ and $\{B_i^r\}$ respectively. Here $B_i = (b_i, c_i) \in \mathbb{R}^4 \times \{1, 2, \cdots, C\}$, b_i and c_i denote the bounding box and the category of the object respectively, and C is the classes number of dataset.

In training stage, all ground-truth labels are given. In inference stage, with different sources of bounding boxes of reference image, we introduce three different settings: (a) **GTBoxR** setting, gives Ground-Truth bounding Boxes $\{B_i^r\}$ of Reference image in inference. Some of the corresponding applications are robotic Pick-and-Place (Zeng et al. 2018) and robot navigation for known scenarios, of which the reference image can be stored and labeled in advance. (b) **PreBoxR** setting, gives Prediction bounding Boxes $\{\hat{B}_i^r\}$ of Reference image in inference. It is suitable for the video-based scenarios, which can reuse the prediction results of the previous frame image. (c) **NoBoxR** setting, gives No bounding Boxes of Reference image in inference. It is more general and challenging than the above settings.

Methodology

We first propose a simple baseline method called MDBase (Match-and-Detection Baseline) network f_{base}, which adopts multi-task paradigm with a shared backbone f_B and two task-heads (i.e. Match Head f_M and Detection Head f_D) for matching and detection. Then, as illustrated in Fig.2, the MatchDet network f_{MD} is constructed upon MDBase network, which additionally inserts three novel modules including Weighted Spatial Attention Module (WSAM) f_{WSAM}, Weighted Attention Module (WAM) f_{WAM} and Box Filter f_{BF}. The WSAM highlights the foreground regions of target image, the WAM enhances the connection between the foreground regions of pair images, and Box Filter mitigates the impact of false matches.

Specifically, let f_B^i be the i^{th} layer of backbone f_B, f_F^i be the i^{th} layer of FPN (Feature Pyramid Network) f_F. Given input image pairs $\{x^t, x^r\}$, the backbone f_B generates corresponding target features $\{C_3^t, C_4^t, C_5^t\}$ and reference features C_3^r respectively, and the FPN f_F further produces target features $\{P_3^t, P_4^t, P_5^t, P_6^t, P_7^t\}$. In particular, the i^{th} layer features C_i^t and C_i^r are produced by f_B^i, and the same goes for other features like P_i^t by f_F^i, where $\{C_i^t, C_i^r, P_i^t\} \in \mathbb{R}^{c_i \times h_i \times w_i}$. Then, WSAM and WAM generate the enhanced features $C_3^{t\prime}$ and $\{\bar{C}_3^t, \bar{C}_3^r\}$ for Detector and Matcher, respectively. Finally, the Match Head f_M and Detection Head f_D predict the homography matrix $\hat{\mathcal{H}}$ and bounding boxes $\{\hat{B}_i^t\}$ for x^t. In detail, the Detection Head f_D is the same as FCOS, and the Match Head f_M is similar to LoFTR which utilizes a dual-softmax matching layer.

MDBase Network

The MDBase network consists of a shared backbone and two task-heads for matching and detection, i.e. $f_{base} = [f_B, f_F, f_M, f_D]$. The MDBase makes predictions as follows:

$$\begin{aligned} \{\hat{B}_i^t\}, \hat{\mathcal{H}} &= f_{base}\left(x^t, x^r\right) \\ where,\ \{\hat{B}_i^t\} &= f_D\left(f_F\left(f_B\left(x^t\right)\right)\right), \\ \hat{\mathcal{H}} &= f_M\left(f_B\left(x^t, x^r\right)\right) \end{aligned} \tag{1}$$

Comparing to the current task-individual solutions, the MDBase network has lower complexity by utilizing a shared backbone. In order to obtain mutual improvements of image matching and object detection, we next introduce a novel MatchDet network benefiting from the collaborative learning of the two tasks.

MatchDet Network

As illustrated in Fig.2, on the basic of MDBase network, the proposed MatchDet integrates Weighted Spatial Attention Module f_{WSAM}, Weighted Attention Module f_{WAM} and

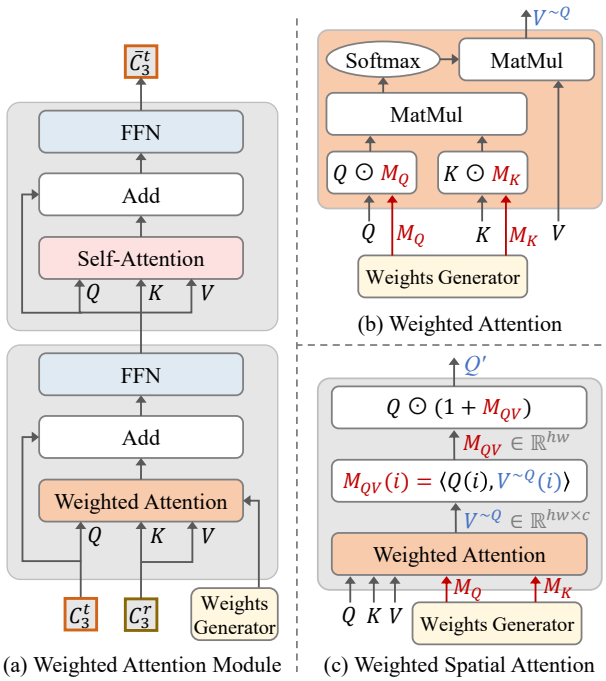

(a) Weighted Attention Module (b) Weighted Attention (c) Weighted Spatial Attention

Figure 3: (a) The Weighted Attention Module (WAM) consists of a Weighted Attention block and a Self-Attention block, where $\{Q, K, V\}$ are known as $\{query, key, value\}$ and FFN denotes Feed-Forward Network in Transformer. (b) The Weighted Attention applied in WAM, where $\odot$ is Broadcasting Element-wise Product. The variables dimensions are $\{V^{\sim Q}, Q, K, V\} \in \mathbb{R}^{hw \times c}$ and $\{M_Q, M_K\} \in \mathbb{R}^{hw}$. (c) The Weighted Spatial Attention enhances the spatial response of Q by $M_{QV} \in \mathbb{R}^{hw}$ to obtain $Q' \in \mathbb{R}^{hw \times c}$, where $\langle \cdot \rangle$ calculates the cosine similarity. And replacing Weighted Attention of WAM with Weighted Spatial Attention derives the Weighted Spatial Attention Module (WSAM).

Figure 4: The visualizations of the generated Weighted Map.

Box Filter f_{BF} to achieve collaborative learning of image matching and object detection tasks. Formally, MatchDet consists of $f_{MD} = [f_{base}, f_{WSAM}, f_{WAM}, f_{BF}]$, and makes predictions as:

$$\begin{aligned} \{\hat{B}_i^t\}, \hat{\mathcal{H}} &= f_{MD}\left(x^t, x^r\right) \\ where,\ \{\hat{B}_i^t\} &= f_D\left(f_F\left(f_{WSAM}(f_B(x^t, x^r))\right)\right), \\ \hat{\mathcal{H}} &= f_M\left(f_{BF}(f_{WAM}(f_B(x^t, x^r)))\right) \end{aligned} \tag{2}$$

In the following, we introduce the detailed structure of the proposed modules and loss function.

Weighted Attention Module The Weighted Attention Module f_{WAM} enhances the connection between the foreground regions of pair images, which is expressed as:

$$\bar{C}_3^t, \bar{C}_3^r = f_{WAM}\left(C_3^t, C_3^r\right), f_{WAM}\left(C_3^r, C_3^t\right) \tag{3}$$

As shown in Fig.3(a), the WAM stacks a Weighted Attention block and a Self-Attention block. Different from the Cross Attention used in LoFTR (Sun et al. 2021) and Masked Attention applied in Mask2Former (Cheng et al. 2022), we propose a novel Weighted Attention as presented in Fig.3(b), which enhances $\{Q, K\}$ with two different weighted maps $\{M_Q, M_K\}$ produced by Weights Generator, respectively. The Weighted Attention operation is formulated as:

$$\begin{aligned} V^{\sim Q} &= \text{WeightedAttention}\left((Q, K, V), M_Q, M_K\right) \\ &= \sigma\left(\left(Q \odot M_Q\right)\left(K \odot M_K\right)^T\right) V \end{aligned} \tag{4}$$

where σ is softmax function. The weighted maps $\{M_Q, M_K\} \in \mathbb{R}^{hw}$ represent the foreground regions of pairs $\{Q, K\}$. Under three different settings introduced in Problem Definition, the Weights Generator of WAM produces different weighted maps $\{M_Q, M_K\}$ as follows:

- **GTBoxR** setting. We denote $\{M_t, M_r\} \in \mathbb{R}^{hw}$ as the foreground regions of $\{C_3^t, C_3^r\}$. In the case of implementing $\bar{C}_3^t = f_{WAM}\left(C_3^t, C_3^r\right)$, there are $M_Q = M_t$ and $M_K = M_r$. Calculating $\bar{C}_3^r = f_{WAM}\left(C_3^r, C_3^t\right)$ assigns $M_Q = M_r$ and $M_K = M_t$. The following assignment rules of $\{M_Q, M_K\}$ with $\{M_t, M_r\}$ are the same, thus we only introduce how to generate $\{M_t, M_r\}$ for simplicity. (a) This setting gives ground-truth $\{B_i^r\}$ for reference image, then we generate M_r by assigning the $\{B_i^r\}$ regions as $1 + \alpha_1$ and other background regions as 1. (b) For target feature C_3^t, we first use a light decoder to predict a semantic segmentation mask m_t. Then we produce M_t by assigning the foreground regions of m_t that are higher than 0.5 as $1 + \alpha_1$, and other background regions as 1. The detail of the light segmentation decoder is described in the following.
- **PreBoxR** setting. Similarly, we use the predicted $\{\hat{B}_i^r\}$ and m_t to generate M_r and M_t, respectively.
- **NoBoxR** setting. The light decoder predicts two semantic segmentation mask m_r and m_t to generate M_r and M_t.

The light segmentation decoder consists of two 3×3 convolution layers and a 1×1 convolution layer, which per-pixel classifies the foreground and background of the image. The light segmentation decoder is optimized by the box-supervised segmentation loss proposed in BoxInst (Tian et al. 2021), which utilizes the ground-truth bounding boxes to supervise the segmentation decoder. Fig.4 presents the generated Weighted Map as the foreground regions.

There are two important abilities of WAM: (a) The features $\{\bar{C}_3^t, \bar{C}_3^r\}$ processed through WAM are more discriminative than $\{C_3^t, C_3^r\}$. The dense local features $\{C_3^t, C_3^r\}$ extracted by Convolutional Neural Networks (CNNs) have limited receptive field which may not distinguish indistinctive or repetitive regions. Transforming by WAM, the global features $\{\bar{C}_3^t, \bar{C}_3^r\}$ have larger global context to find the correspondences among surrounding regions. (b) The WAM enhances the connection between foreground regions with the constrained of $\{M_Q, M_K\}$, which benefits the subsequent matching layer to obtain high-quality matches. The Cross

Attention in Transformer learns global context based on the affinity matrix between feature pairs, which may easily to be disturbed by background noise and leads to false matches. With the constrained of $\{M_Q, M_K\}$, the WAM can be more focus on interacting information among the foreground regions to ensure high-quality matches.

Weighted Spatial Attention Module The Weighted Spatial Attention Module f_{WSAM} highlights the foreground regions of target image, which is expressed as:

$$C_3^{t\prime} = f_{WSAM}\left(C_3^t, C_3^r\right) \tag{5}$$

The WSAM stacks a Weighted Spatial Attention block and a Self-Attention block. And the structure of the key component Weighted Spatial Attention (WSAttention) is illustrated in Fig.3(c), which is formulated as:

$$\begin{aligned} Q' &= \text{WSAttention}\left((Q,K,V), M_Q, M_K\right) \\ &= Q \odot (1 + M_{QV}) \\ &where,\ M_{QV}(i) = \langle Q(i), V^{\sim Q}(i)\rangle, \\ V^{\sim Q} &= \text{WeightedAttention}\left((Q,K,V), M_Q, M_K\right) \end{aligned} \tag{6}$$

Here we explain the meanings of key variables in Weighted Spatial Attention: (a) The $V^{\sim Q}$, is Q-aligned V, i.e. aggregates V into alignment with Q. At i^{th} spatial position, $V^{\sim Q}(i)$ is aggregated from V with the affinity vector between $(Q(i), K)$. Intuitively, $V^{\sim Q}(i)$ collects all the patch features from V that are semantically similar to $Q(i)$. (b) Q', is M_{QV}-enhanced Q, i.e. uses the cosine similarity map M_{QV} between $(Q, V^{\sim Q})$ to re-weight Q. Therefore, Q' will be enhanced if Q is similar to $V^{\sim Q}$ (i.e. Q-aligned V). Thus Weighted Spatial Attention is able to enhance the spatial response of Q via the similar regions with V.

Based on the above analysis, we propose to use instance feature C_3^r and learnable semantic embedding $W_e \in \mathbb{R}^{C\times c_3}$ (i.e. pytorch code is W_e=nn.Embedding(C, c_3)) to highlight C_3^t, i.e. C_3^t can be highlighted by the similar regions of C_3^r and W_e, where W_e contains foreground semantics via learning all categories information (Lai et al. 2022). Formally,

$$\begin{aligned} Q' = &\text{WSAttention}\left(\left(C_3^t, C_3^r, C_3^r\right), M_Q, M_K\right) \\ &+ \text{WSAttention}\left(C_3^t, W_e, W_e\right) \end{aligned} \tag{7}$$

The WSAM needs to find the foreground regions of C_3^r to highlight C_3^t. Under different settings, the Weights Generator of WSAM produces different weighted maps $\{M_Q, M_K\}$=$\{M_t, M_r\}$ (i.e. the potential foreground regions of $\{C_3^t, C_3^r\}$) as follows:

• **GTBoxR** setting. For C_3^r, we generate M_r by assigning the given ground-truth $\{B_i^r\}$ regions as $1+\alpha_2$ and other background regions as 1. For C_3^t, we use the estimated homography $\mathcal{H}'$ = $f_M\left(f_{WAM}\left(f_B\left(x^t, x^r\right)\right)\right)$ to affine M_r to generate M_t = $\mathcal{H}'M_r$.

• **PreBoxR** setting. Similarly, we use the predicted $\{\hat{B}_i^r\}$ to generate M_r, and then obtains M_t = $\mathcal{H}'M_r$.

• **NoBoxR** setting. Firstly, the light decoder predicts two semantic segmentation mask m_r and m_t to generate M_r and M_t, respectively. Then we further refine the maps by M_r = $M_r + \mathcal{H}'^{-1}M_t$ and M_t = $M_t + \mathcal{H}'M_r$.

Match Head with Box Filter **Box Filter** f_{BF} produces an filter map $\mathcal{F}$ to mitigate the impact of false matches measured by $\mathcal{H}'$ = $f_M\left(f_{WAM}\left(f_B\left(x^t, x^r\right)\right)\right)$ on stage ②. After stage ③, Detector branch outputs the prediction boxes $\{\hat{B}_i^t\}$. On stage ④, we first generate foreground regions $\hat{M}_t$ of target image by assigning $\{\hat{B}_i^t\}$ regions as $1+\beta$ and other background regions as 1, and then we obtain the foreground $\hat{M}_r$ of reference image from WSAM with M_r of which foreground is also re-assigned as $1+\beta$. Finally, filter map $\mathcal{F}$ is generated by $\mathcal{F}(i,j) = \hat{M}_t(i)\cdot\hat{M}_r(j)$.

Match Head f_M is based on the dual-softmax matching layer (Tyszkiewicz, Fua, and Trulls 2020; Sun et al. 2021). Formally, the matching probability $\mathcal{P}$ is obtained by:

$$\begin{aligned} \mathcal{P}(i,j) &= \sigma\left(\mathcal{S}\left(i,\cdot\right)\right)_j \cdot \sigma\left(\mathcal{S}\left(\cdot,j\right)\right)_i, \\ where,\ \mathcal{S}\left(i,j\right) &= \frac{1}{\tau}\cdot\langle \bar{C}_3^t(i), \bar{C}_3^r(j)\rangle \end{aligned} \tag{8}$$

where $\mathcal{S}$ is the score matrix between the feature pairs $(\bar{C}_3^t, \bar{C}_3^r)$. The dual-softmax matching applies softmax on both dimensions of $\mathcal{S}$ to obtain the matching probability $\mathcal{P}$. Then, we use the filter map $\mathcal{F}$ generated by Box Filter to update $\mathcal{P}$ by $\mathcal{P}(i,j) \leftarrow \mathcal{P}(i,j)\cdot\mathcal{F}(i,j)$. Next, we obtain the match prediction by $\hat{\mathcal{M}} = \{\left(\tilde{i},\tilde{j}\right) \mid \forall\left(\tilde{i},\tilde{j}\right) \in \text{MNN}\left(\mathcal{P}\right),\ \mathcal{P}\left(\tilde{i},\tilde{j}\right) \geq \theta\}$, where, MNN is a Mutual Nearest Neighbor operator, and θ is a threshold to select good matches. Finally, the homography matrix is estimate by RANSAC algorithm with $\hat{\mathcal{H}} = \text{RANSAC}(\hat{\mathcal{M}})$.

Loss Function The MatchDet network is optimized by the loss function: $\mathcal{L} = \mathcal{L}_{matcher} + \lambda\mathcal{L}_{detector}$, where $\mathcal{L}_{matcher}$ and $\mathcal{L}_{detector}$ are the losses of Matcher branch and Detector branch respectively, and λ is the balance weight. The $\mathcal{L}_{detector}$ is the same as FCOS (Tian et al. 2019). Following LoFTR (Sun et al. 2021), the $\mathcal{L}_{matcher}$ is formulated as: $\mathcal{L}_{matcher} = -\frac{1}{|\mathcal{M}|}\sum_{(\tilde{i},\tilde{j})\in\mathcal{M}}\log\hat{\mathcal{M}}\left(\tilde{i},\tilde{j}\right)$, where $\mathcal{M}$ and $\hat{\mathcal{M}}$ are ground-truth and predicted matches.

Discussion

Task-collaborative vs. Task-individual Comparing to the current task-individual solutions, the advantages of our task-collaborative framework MatchDet are: (a) With the collaborative learning of image matching and object detection tasks, MatchDet is able to obtain mutual performance improvements. (b) Lower complexity with a shared backbone. (c) More convenient in practical applications with one single MatchDet model for two tasks.

WSAM vs. WAM The WAM transforms the pair features of target and reference images into new feature space that are easy to measure similarity for matching, while the WSAM utilizes a spatial map to enhance the foregrounds of target image for detection. Details are presented in APPENDIX.

Weighted Attention vs. Masked Attention The proposed Weighted Attention has three main differences from Masked Attention (Cheng et al. 2022), including input forms, weighting operation, and weights generation. These

{Target image, Reference image}	Method	*Average Precision* on Target image						Homography est. AUC			Params	FLOPs
		AP	AP_{50}	AP_{75}	AP_S	AP_M	AP_L	@3px	@5px	@10px		
{Warp-COCO, COCO}	FCOS (Tian et al. 2019)	31.02	47.99	33.08	11.09	28.10	43.66	-	-	-	32.29M	174604M
	LoFTR (Sun et al. 2021)	-	-	-	-	-	-	47.94	68.15	84.02	27.67M	171076M
	DBase	30.94	47.65	32.66	10.82	27.76	43.32	-	-	-	32.29M	174604M
	MBase	-	-	-	-	-	-	38.94	58.67	78.39	23.51M	143340M
	MDBase	30.95	47.57	32.67	11.23	27.50	43.48	36.42	56.78	77.32	32.29M	206641M
	MatchDet-G	**43.62**	**61.66**	**47.32**	**19.71**	**41.90**	**56.74**	**63.18**	**77.86**	**89.02**	38.54M	248246M
	MatchDet-P	34.15	51.23	35.98	14.79	31.19	46.13	58.31	73.54	83.24	38.54M	248246M
	MatchDet-N	32.28	49.28	34.01	12.81	29.40	44.38	54.11	69.06	79.82	38.54M	257154M
{miniScanNet-F0, miniScanNet-F1}	FCOS (Tian et al. 2019)	25.13	39.56	25.63	0.26	4.43	29.67	-	-	-	32.15M	60709M
	LoFTR (Sun et al. 2021)	-	-	-	-	-	-	10.75	31.48	50.02	27.67M	69729M
	DBase	24.99	39.22	25.50	0.24	4.39	29.52	-	-	-	32.15M	60709M
	MBase	-	-	-	-	-	-	5.87	16.34	33.66	23.51M	50590M
	MDBase	23.70	38.05	23.60	0.25	3.46	28.15	5.95	16.50	33.93	32.15M	72016M
	MatchDet-G	**40.69**	**58.12**	**41.38**	**1.88**	**25.76**	**45.03**	**18.43**	**39.14**	**57.11**	38.39M	100725M
	MatchDet-P	28.29	43.12	29.34	0.82	6.54	33.03	14.39	35.18	53.24	38.39M	100725M
	MatchDet-N	27.33	42.09	27.58	0.56	5.47	32.29	12.47	33.09	51.32	38.39M	104289M

Table 1: MatchDet vs. other methods on different combinations of {Target image, Reference image} pairs on Full Warp-COCO and miniScanNet datasets. The *Average Precision* on Target image, homography estimation AUC of the corner error in percentage, epochs=12, params and FLOPs are reported. The DBase = $[f_B, f_F, f_D]$ and MBase = $[f_B, f_M]$ are detector network and matcher network split from MDBase, respectively. The MatchDet-G, MatchDet-P and MatchDet-N follow three different settings of **GTBoxR**, **PreBoxR** and **NoBoxR**, respectively.

Method	*Ave. Precision*			Homo. est. AUC		
	AP	AP_{50}	AP_{75}	@3px	@5px	@10px
LoFTR	-	-	-	45.88	65.15	84.99
FCOS	37.32	55.69	40.37	-	-	-
DBase(FC)	37.19	55.54	39.96	-	-	-
MBase	-	-	-	34.86	54.25	74.91
MDBase(FC)	37.07	55.38	39.68	32.67	52.76	73.24
MatchDet-G(FC)	**43.99**	**61.93**	**47.75**	**60.09**	**74.58**	**86.07**
MatchDet-P(FC)	40.57	58.66	42.39	55.21	70.32	80.17
MatchDet-N(FC)	39.49	57.47	41.25	51.24	66.12	76.79
Faster-RCNN	35.90	56.28	39.05	-	-	-
MatchDet-G(FR)	**42.22**	**62.44**	**45.98**	**68.72**	**80.83**	**90.37**
MatchDet-P(FR)	39.79	60.13	43.29	65.13	79.02	87.56
MatchDet-N(FR)	37.85	58.72	41.55	62.37	76.43	85.68
AdaMixer	40.82	59.72	43.73	-	-	-
MatchDet-G(AM)	**48.19**	**66.57**	**52.35**	**68.88**	**80.96**	**90.96**
MatchDet-P(AM)	45.01	64.35	49.23	65.21	78.53	88.55
MatchDet-N(AM)	42.19	62.52	46.22	62.74	76.69	86.88

Table 2: The results of our MatchDet with different detectors, on {COCO,Warp-COCO}. The FC, FR, and AM represent FCOS, Faster-RCNN, and AdaMixer, respectively.

differences make Masked Attention can not be directly integrated by our MatchDet. Masked Attention performs cross-attention between input features and learnable embedding, while Weighted Attention processes a pair of features. Due to this difference in input forms, Weighted Attention needs to generate two corresponding weighted maps for feature pairs. Besides, Mask2Former is applied in segmentation task with the supervision of ground-truth masks, which is easy to obtain good quality masks for Masked Attention. While our MatchDet is proposed for detection task with ground-truth bounding boxes only, thus we propose a Weights Generator using the weakly-supervised segmentation technique to generate coarse masks for Weighted Attention.

Method	Modules			*Ave. Precision*		Homo. est. AUC		
	A.	S.	B.	AP	AP_{50}	@3px	@5px	@10px
MDBase	-	-	-	30.95	47.57	36.42	56.78	77.32
MatchDet-G	✓			30.66	47.25	60.12	74.92	87.01
MatchDet-G	✓	✓		**43.62**	**61.66**	61.15	75.95	87.92
MatchDet-G	✓	✓	✓	**43.62**	**61.66**	**63.18**	**77.86**	**89.02**
MatchDet-P	✓			30.69	47.27	55.43	70.49	81.54
MatchDet-P	✓	✓		**34.15**	**51.23**	56.42	71.48	82.35
MatchDet-P	✓	✓	✓	**34.15**	**51.23**	**58.31**	**73.54**	**83.24**
MatchDet-N	✓			30.60	47.21	51.67	66.52	78.20
MatchDet-N	✓	✓		**32.28**	**49.28**	52.43	67.49	79.02
MatchDet-N	✓	✓	✓	**32.28**	**49.28**	**54.11**	**69.06**	**79.82**

Table 3: The influence of WAM (A.), WSAM (S.) and Box Filter (B.) on {Warp-COCO,COCO} pairs dataset.

Experiments

Datasets

Warp-COCO The Full Warp-COCO dataset consists of Warp-COCO and COCO (Lin et al. 2014), i.e. every image in COCO has a corresponding transformed synthetic image to make a pair, which has ground-truth poses and boxes.

miniScanNet We selected 20 categories from ScanNet (Dai et al. 2017) dataset (230M image pairs) with high-quality bounding boxes to make a new miniScanNet dataset (188K image pairs), which is 1000 times smaller than ScanNet. The miniScanNet consists of real-world image pairs, which is more challenging than the synthetic Warp-COCO dataset.

Evaluation Metrics and Implementation Details

The *Average Precision* (AP) and the Area Under the Cumulative curve (AUC) of the corner error, are used for object

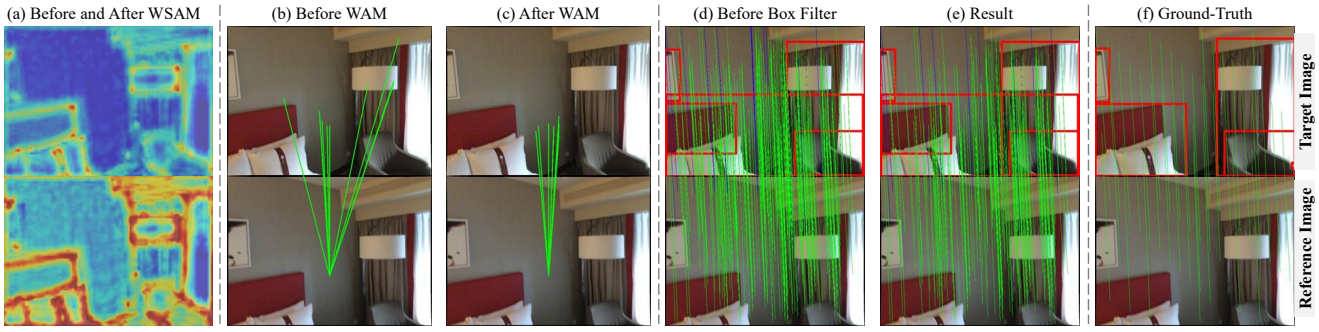

Figure 5: The visualizations for WAM, WSAM, Box Filter and MatchDet results under **GTBoxR** setting from miniScanNet. (a) - (e), are the results processed by the corresponding modules before and after, respectively. (e) shows the predicted bounding boxes and matching results of MatchDet, where these matches are obtained after Box Filter. (f) is Ground-Truth.

f_{WAM}	f_{WSAM}	*Average Precision*			Homography est. AUC		
		AP	AP_{50}	AP_{75}	@3px	@5px	@10px
C.A.	C.A.	31.01	47.72	32.91	45.84	66.13	82.89
W.A.	W.A.	40.41	58.43	44.21	60.03	74.88	86.99
W.S.A.	W.S.A.	42.13	60.07	46.00	58.46	73.40	86.08
W.S.A.	W.A.	40.02	58.00	43.86	57.88	72.89	85.66
W.A.	W.S.A.	**43.62**	**61.66**	**47.32**	**61.15**	**75.95**	**87.92**

Table 4: The influence of Weighted Attention (W.A.) and Weighted Spatial Attention (W.S.A.), under **GTBoxR** setting on {Warp-COCO,COCO} pairs dataset. The f_{WAM} and f_{WSAM} are inserted into Matcher and Detector respectively, i.e. f_{WAM} and f_{WSAM} directly affect the AUC and the AP respectively. We give different combinations of Cross Attention (C.A.), W.A. and W.S.A.

detection and image matching, respectively. The used backbone is ResNet-50 (He et al. 2016). The data augmentation is not applied for all methods. The hyper-parameters are set as $\alpha_1 = 1.0$, $\alpha_2 = 1.0$, $\beta = 1.0$, $\lambda = 1.0$.

Comparison with Related Methods

As shown in Tab.1 and Tab.2, we conduct experiments on Full Warp-COCO and miniScanNet datasets with different combinations of {Target image, Reference image} pairs, including {Warp-COCO, COCO}, {COCO, Warp-COCO} and {miniScanNet-F0, miniScanNet-F1}. The DBase and MBase are the two task-individual baselines for object detection and image matching, respectively. The MDBase is the task-collaborative baseline for Match-and-Detection task, which obtains similar AP and AUC compared to DBase and MBase respectively. Under three different settings of **GTBoxR**, **PreBoxR** and **NoBoxR**, our MatchDet outperforms these baselines on both AP and AUC performances, which demonstrates that the proposed approaches can achieve the collaborative learning between matching and detection tasks to obtain mutual performance improvements. Under the **GTBoxR** setting, MatchDet obtains a larger performance improvement. Even under the most challenging **NoBoxR** setting, our MatchDet still achieves competitive improvement.

Ablation Study

WAM, WSAM and Box Filter. The results in Tab.3 demonstrate that the proposed three modules achieve consistent improvements under the settings of **GTBoxR**, **PreBoxR** and **NoBoxR**. Specifically, the WSAM highlights the foreground regions of target image to boost the AP of detection task. The WAM and Box Filter obtains high-quality matches to improve the AUC of image matching task.

Weighted Attention and Weighted Spatial Attention. The results in Tab.4 show that: (a) The best setting is using Weighted Attention for Matcher and Weighted Spatial Attention for Detector. These experimental results coincide with the theoretical analysis in AAPPENDIX. (b) The proposed Weighted Attention and Weighted Spatial Attention, exploring the correlation between foreground regions of feature pairs, are able to obtain better performance than the traditional Cross Attention.

Visualization Analysis

Fig.5 shows the visualizations for WAM, WSAM, Box Filter and MatchDet results under **GTBoxR** setting. Fig.5(a) shows that the WSAM is able to highlight the foreground regions. Comparing Fig.5(c) to Fig.5(b), the WAM finds the correspondences among surrounding regions to produce more discriminative feature representations. Comparing Fig.5(e) to Fig.5(d), Box Filter reduces the background interference to obtain high-quality matches.

Conclusion

In this paper, we propose a collaborative framework called MatchDet for image matching and object detection to obtain mutual improvements. To achieve the collaborative learning of the two tasks, three novel modules are proposed, including a Weighted Spatial Attention Module (WSAM) which highlights the foreground regions of target image for Detector, and Weighted Attention Module (WAM) and Box Filter which obtains high-quality matches for Matcher. The experimental results on Warp-COCO and miniScanNet datasets show that our approaches are effective and achieve competitive improvements.

References

Carion, N.; Massa, F.; Synnaeve, G.; Usunier, N.; Kirillov, A.; and Zagoruyko, S. 2020. End-to-end object detection with transformers. In *ECCV*.

Chen, Y.; Huang, D.; Xu, S.; Liu, J.; and Liu, Y. 2022. Guide local feature matching by overlap estimation. In *AAAI*.

Cheng, B.; Misra, I.; Schwing, A. G.; Kirillov, A.; and Girdhar, R. 2022. Masked-attention mask transformer for universal image segmentation. In *CVPR*.

Christoph, F.; Axel, P.; and Andrew, Z. 2017. Detect to track and track to detect. In *ICCV*.

Dai, A.; Chang, A. X.; Savva, M.; Halber, M.; Funkhouser, T.; and Nießner, M. 2017. Scannet: Richly-annotated 3d reconstructions of indoor scenes. In *CVPR*, 5828–5839.

DeTone, D.; Malisiewicz, T.; and Rabinovich, A. 2018. Superpoint: Self-supervised interest point detection and description. In *CVPR workshops*, 224–236.

Duan, K.; Bai, S.; Xie, L.; Qi, H.; Huang, Q.; and Tian, Q. 2019. Centernet: Keypoint triplets for object detection. In *ICCV*.

Gao, Z.; Wang, L.; Han, B.; and Guo, S. 2022. Adamixer: A fast-converging query-based object detector. In *CVPR*.

He, K.; Zhang, X.; Ren, S.; and Sun, J. 2016. Deep residual learning for image recognition. In *CVPR*.

Huang, D.; Chen, Y.; Liu, Y.; Liu, J.; Xu, S.; Wu, W.; Ding, Y.; Tang, F.; and Wang, C. 2023. Adaptive assignment for geometry aware local feature matching. In *CVPR*.

Lai, J.; Yang, S.; Liu, W.; Zeng, Y.; Huang, Z.; Wu, W.; Liu, J.; Gao, B.-B.; and Wang, C. 2022. tSF: Transformer-Based Semantic Filter for Few-Shot Learning. In *ECCV*.

Law, H.; and Deng, J. 2018. Cornernet: Detecting objects as paired keypoints. In *ECCV*.

Lin, T.-Y.; Goyal, P.; Girshick, R.; He, K.; and Dollár, P. 2017. Focal loss for dense object detection. In *ICCV*.

Lin, T.-Y.; Maire, M.; Belongie, S.; Hays, J.; Perona, P.; Ramanan, D.; Dollár, P.; and Zitnick, C. L. 2014. Microsoft coco: Common objects in context. In *ECCV*.

Liu, L.; Ouyang, W.; Wang, X.; Fieguth, P.; Chen, J.; Liu, X.; and Pietikäinen, M. 2020. Deep learning for generic object detection: A survey. *IJCV*, 128(2): 261–318.

Mur-Artal, R.; Montiel, J. M. M.; and Tardos, J. D. 2015. ORB-SLAM: a versatile and accurate monocular SLAM system. *IEEE transactions on robotics*, 31(5): 1147–1163.

Redmon, J.; and Farhadi, A. 2018. Yolov3: An incremental improvement. *arXiv preprint arXiv:1804.02767*.

Ren, S.; He, K.; Girshick, R.; and Sun, J. 2015. Faster R-CNN: Towards real-time object detection with region proposal networks. In *NeurIPS*.

Rublee, E.; Rabaud, V.; Konolige, K.; and Bradski, G. 2011. ORB: An efficient alternative to SIFT or SURF. In *ICCV*, 2564–2571.

Shrivastava, A.; Malisiewicz, T.; Gupta, A.; and Efros, A. A. 2011. Data-driven visual similarity for cross-domain image matching. In *SIGGRAPH*, 1–10.

Sun, J.; Shen, Z.; Wang, Y.; Bao, H.; and Zhou, X. 2021. LoFTR: Detector-free local feature matching with transformers. In *CVPR*, 8922–8931.

Tian, Z.; Shen, C.; Chen, H.; and He, T. 2019. Fcos: Fully convolutional one-stage object detection. In *ICCV*, 9627–9636.

Tian, Z.; Shen, C.; Wang, X.; and Chen, H. 2021. Boxinst: High-performance instance segmentation with box annotations. In *CVPR*.

Tyszkiewicz, M. J.; Fua, P.; and Trulls, E. 2020. DISK: Learning local features with policy gradient. In *NeurIPS*.

Zeng, A.; Song, S.; Yu, K.-T.; Donlon, E.; Hogan, F. R.; Bauza, M.; Ma, D.; Taylor, O.; Liu, M.; Romo, E.; Fazeli, N.; Alet, F.; Dafle, N. C.; Holladay, R.; Morona, I.; Nair, P. Q.; Green, D.; Taylor, I.; Liu, W.; Funkhouser, T.; and Rodriguez, A. 2018. Robotic Pick-and-Place of Novel Objects in Clutter with Multi-Affordance Grasping and Cross-Domain Image Matching. In *ICRA*.

Zhang, H.; Li, F.; Liu, S.; Zhang, L.; Su, H.; Zhu, J.; Ni, L. M.; and Shum, H.-Y. 2023. Dino: Detr with improved denoising anchor boxes for end-to-end object detection. *ICLR*.

Zhang, S.; Chi, C.; Yao, Y.; Lei, Z.; and Li, S. Z. 2020. Bridging the gap between anchor-based and anchor-free detection via adaptive training sample selection. In *CVPR*.

Zhang, X.; Wan, F.; Liu, C.; Ji, R.; and Ye, Q. 2019. Freeanchor: Learning to match anchors for visual object detection. In *NeurIPS*.